https://doi.org/10.3311/PPch.41785

Periodica Polytechnica Chemical Engineering, 69(4), pp. 685–696, 2025

Maximizing Lithium–Air Battery Performance with Polystyrene Based Membranes in Humid Environments

Asad A. Naqvi[1*], Awan Zahoor[2]

[1] Department of Mechanical Engineering, NED University of Engineering and Technology, Karachi, Pakistan
[2] Department of Food Engineering, NED University of Engineering and Technology, Karachi, Pakistan
[*] Corresponding author, e-mail: asadakhter@cloud.neduet.edu.pk

Received: 30 July 2025, Accepted: 03 October 2025, Published online: 04 November 2025

Abstract

The lithium–air battery (LAB) is considered the most promising battery type due to its significantly high theoretical energy density, which is comparable to that of gasoline. Most LAB research takes place in pure oxygen environments, as operating them under normal conditions with moisture raises safety concerns. This study focuses on creating polystyrene (PS) based membranes with added graphite to enhance their properties. The quantity of graphite ranges from 0 to 1 wt.% of PS, and the resulting membrane undergoes characterization using Fourier transform infrared spectroscopy (FTIR), X-ray diffractometry (XRD), scanning electron microscopy (SEM), water contact angle (WCA), and moisture transmission rate (MTR). The investigation reveals that the 0.7 wt.% graphite infused PS membrane performs efficiently and is subsequently employed in LAB. Additionally, the use of MnO_2 as a catalyst in the cathode material is explored through cyclic voltammetry (CV) and electrochemical impedance spectroscopy (EIS), showing promising results. When tested in a moist gas environment alongside the optimal membrane, the LAB behaves similarly to LAB without a membrane, akin to its performance in a pure oxygen setting.

Keywords

lithium–air battery, hydrophobic membranes, water contact angle, charge discharge test, polystyrene

1 Introduction

Due to the increasing popularity of electric vehicles (EVs), rechargeable batteries have garnered significant attention. While lead-acid and lithium–ion batteries are commonly used in vehicles, they struggle to compete with gasoline due to their lower specific energy when compared to gasoline [1]. Among all battery types, lithium–air batteries (LABs) stand out with the highest specific energy of 11,900 Wh/kg, nearly on par with gasoline at 12,700 Wh/kg [2]. The pioneering work on such batteries is reported by Abraham and Jiang [3]. Fig. 1 illustrates the scheme of a LAB, depicting its components: pure lithium metal as the anode, a porous cathode made of carbon based materials and an organic electrolyte. During discharge lithium ions migrate through the electrolyte, while electrons traverse the external circuit, ultimately combining with oxygen at the cathode to form Li_2O_2, thereby generating electricity. Charging, on the other hand, involves the decomposition of Li_2O_2 into Li and oxygen through the application of electrical current. The discharging and charging processes are governed by Eqs. (1) and (2) [4, 5].

During discharging

$$2Li + O_2 \rightarrow Li_2O_2 \tag{1}$$

During charging

$$Li_2O_2 \rightarrow 2Li + O_2 \tag{2}$$

Most of the research on LAB is performed in pure oxygen [6–15]. The use of oxygen includes issues like the additional mass of the cylinder, and the refilling of the cylinder, and will also have some serious safety hazards [16]. The more practical approach to running LAB is the use of ambient air for the supply of oxygen, but apart of oxygen, ambient air also includes nitrogen, carbon dioxide, and some traces of moisture [17]. Lithium metal is very sensitive to moisture [18]. On contact with moisture, it will form lithium hydroxide through an exothermic reaction [16] which is considered to be a safety concern [1].

Huang et al. [19] evaluated that when LAB is discharged in ambient air, the discharge product Li_2O_2 reacts with moisture and carbon dioxide, which is difficult to decompose.

Cite this article as: Naqvi, A. A., Zahoor, A. "Maximizing Lithium–Air Battery Performance with Polystyrene Based Membranes in Humid Environments", Periodica Polytechnica Chemical Engineering, 69(4), pp. 685–696, 2025. https://doi.org/10.3311/PPch.41785

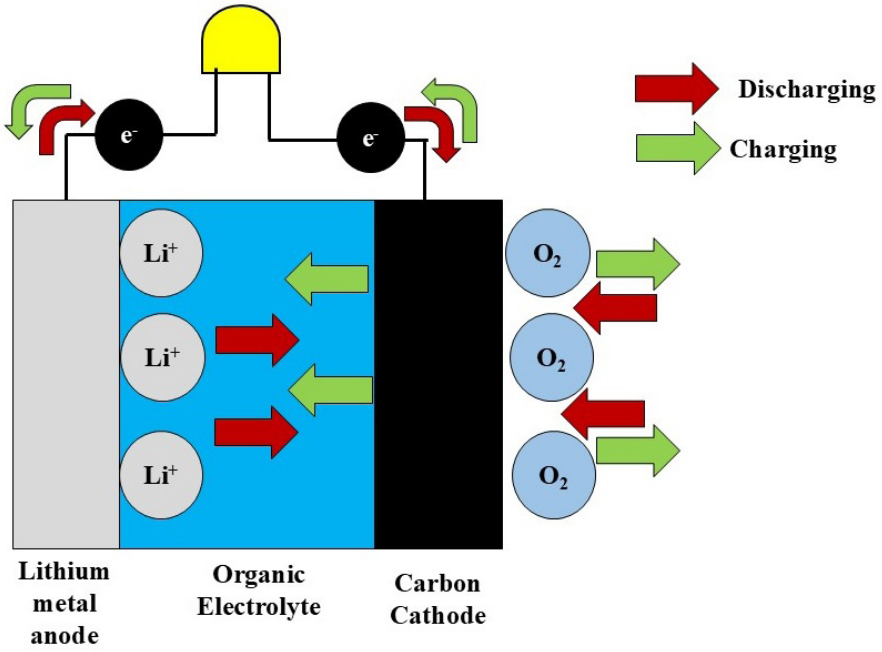

Fig. 1 Scheme of conventional lithium-air battery

The attractive option to operate the LAB in an ambient atmosphere is the use of hydrophobic membranes [20], which should block moisture and allow only oxygen into the battery. Muthiah et al. [21] initially proposed the idea of using a Teflon based membrane to prevent moisture from entering the battery, but they did not conduct an assessment of the battery performance with this membrane. In a subsequent study, Crowther and Salomon [22] employed a Teflon-coated fiberglass cloth membrane to block moisture and allow the ambient operation of LAB. They observed a 94% increase in battery capacity when LAB was operated with this membrane under ambient conditions compared to operation without the membrane. Another investigation by Zhang et al. [23] involved experimental testing of a heat-sealed polymer as a moisture-blocking membrane and for battery packaging. Their findings indicated that using this membrane along with the battery could achieve a capacity of 362 Wh/kg while operating in ambient conditions. Zou et al. [24] used silica gel based oxygen selective membrane (OSM) for blocking moisture. They tested the battery in dry and humid air. They experimentally evaluated that LAB can be run for 165 cycles in dry air by discharging at a rate of 0.5 A/g, while LAB has provided only 12 cycles when operated in the air with 45% relative humidity (RH). When a silica gel based membrane is used for moisture blocking, LAB is able to run for 130 cycles at the same rate. They have also evaluated that LiOH is the main discharge product when the battery is operated without a membrane while Li_2O_2 is mainly observed as a discharged product when the battery is operated along with the membrane. Xie et al. [25] have synthesized perfluoropolyether based OSM and evaluated that the membrane has a hydrophobic nature. They tested the membrane for the ambient operation of LAB and concluded that a battery equipped with a membrane can be run for 144 cycles and can provide 500 mAh/g while a battery without a membrane is only able to provide 6 cycles. Zhang et al. [26] have prepared OSM by using silicate zeolite and polytetrafluoroethylene and tested the membrane in a battery. It is found that while operating the battery with the membrane in 20% RH battery could provide 1022 mAh/g and can run for 21 days. Fu et al. [27] tested the LAB in 20% RH at a discharge rate of 0.1 mA/g by using a membrane made of polyaniline (PANI). It was found that the battery can deliver 3240 mAh/g without any safety issues as PANI membrane can block the moisture. Wen et al. [28] prepared a polytetrafluoroethylene hexafluoropropylene (PVDF-HFP) based membrane and utilized it as OSM in LAB, it was found during their investigation that the use of membrane improved the battery performance by 8 times, when the battery was tested in 50 RH. The use of a polydimethylsiloxane (PDMS) based OSM was tested by Wang et al. [29] in which SiO_2 was used as nano-particles The membrane was tested to operate the battery in ambient conditions. It was found that the battery could provide 500 mAh/g up to 20 cycles when operated at 40% RH.

Based on the preceding discussion, it becomes evident that hydrophobic membranes proved to be highly effective at preventing moisture infiltration, thereby enabling the

operation of LAB under regular environmental conditions. Although various polymeric membranes have been assessed for LAB operation under ambient conditions, to the best of the authors' knowledge, using polystyrene (PS) based membranes in LAB for ensuring secure ambient operation has not been explored. This research focused on the utilization of LAB under humid conditions by using PS membranes. The oxygen selectivity and hydrophobicity of the PS membranes were tried to be improved by incorporating graphite nanoflakes, and the quantity of graphite flakes in the PS membranes was optimized. Moreover, battery testing with the membrane was also conducted to explore the impact of the optimized membrane on battery performance.

2 Methodology

The overall study was conducted according to the flow presented in Fig. 2. It began with the synthesis of PS membranes with and without fillers. Characterization of the synthesized membranes was performed to evaluate the physical and chemical properties, and the best performing candidates were selected. Batteries were assembled and tested with and without the use of membranes to compare their performance.

2.1 Materials

PS (resin), toluene (reagent grade), graphite powder, and Nafion binder were taken from Sigma Aldrich. Ethanol, carbon black, and MnO_2 were taken from Lab Chem Products.

2.2 Membrane synthesis

Five different membranes having PS as base matrix with varying compositions of graphite (G) were synthesized by solution casting technique. The quantity of graphite varied from 0 to 1 wt.% of PS. Pristine PS membrane was prepared by making a solution of PS and toluene such that the mass ratio of PS and toluene was 2:10. The solution was then poured on the plastic sheet placed on the applicator and its thickness is controlled by a doctor blade.

Fig. 3 illustrates the scheme of the graphite infused membrane. To create this membrane, 0.3 wt.% of PS and graphite were combined in toluene. The mixture underwent 30 min ultrasonication to ensure a uniform distribution of graphite within the toluene. Subsequently, PS resin is introduced into the mixture, aiming for a mass ratio of PS and toluene as 2:10. To achieve a consistent blend of PS in toluene the mixture is subjected to magnetic stirring for 1 h. The resulting solution is then poured onto a plastic sheet positioned on an applicator, with the thickness being regulated using a doctor blade. Afterward, the sample is left to dry for 24 h, rendering the membrane ready for use. The same procedure is employed for the creation of graphite filled PS membranes with concentrations of 0.5 wt.%, 0.7 wt.%, and 1 wt.%.

2.3 Battery assembly

The battery was assembled in an argon filled glove box. Lithium coin was used as anode, the cathode was made

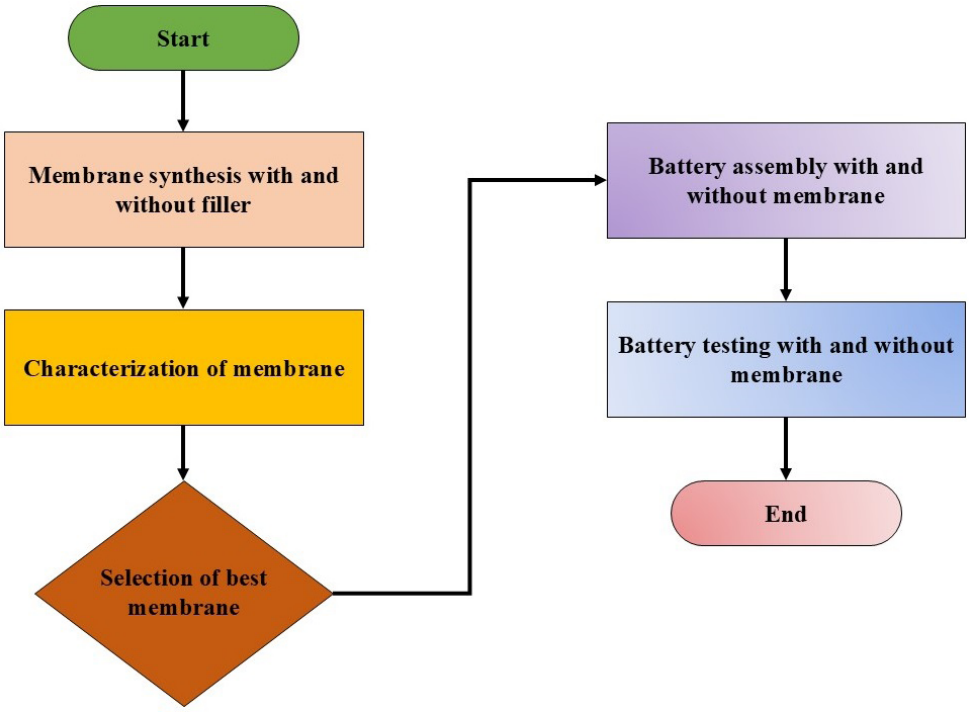

Fig 2 Workflow adapted for this study

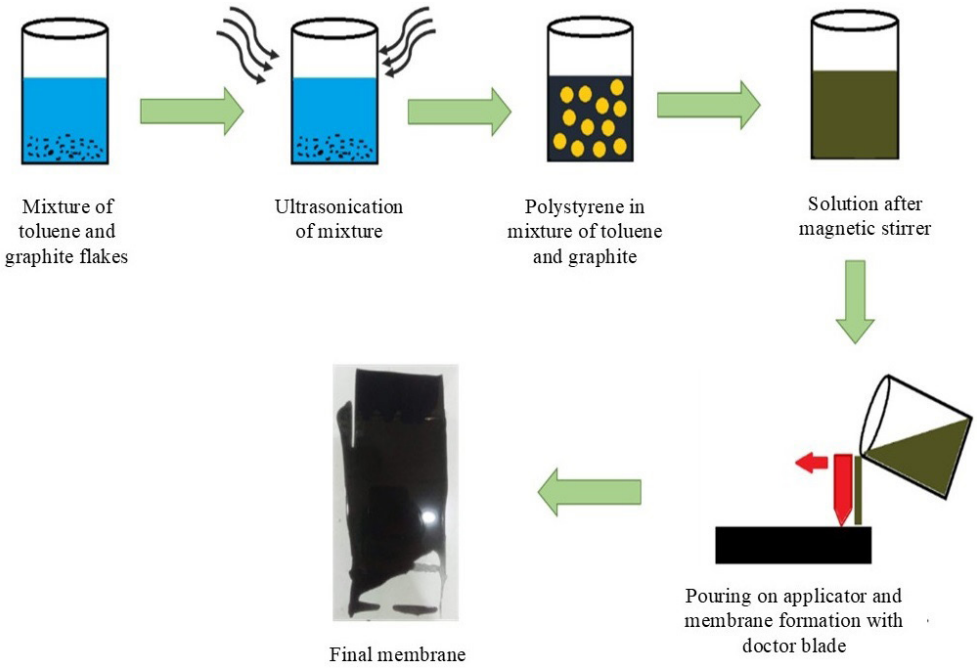

Fig. 3 Preparation of graphite-filled PS membrane

of carbon along with MnO_2 bonded over a nickel mesh. A solution of LiF and polypropylene was prepared as electrolyte such that the LiF concentration in the solution was 0.6 M. The cathode was prepared by making a slurry of 5 mg carbon black, 5 mg MnO_2, 10 mL distilled water and 10 mL ethanol. 3.5 µm PTFE resin was added as a binder to the mixture and then this mixture (slurry) was deposited on nickel mesh and then left for drying for 24 h. Polyvinylidene fluoride (PVDF) was used as separating material to avoid any physical contact between the cathode and anode. The membrane was placed over the cathode to avoid the interaction of moisture with the cathode. The scheme of the battery with the membrane is presented in Fig. 4. The membrane blocks the moisture and only oxygen can get into the battery.

2.4 Membrane characterization and electrochemical evaluation of battery

The prepared membranes underwent several characterization techniques for analysis. Fourier transform infrared spectroscopy (FTIR) was employed to examine the membrane functionality through NICOLET IS50, X-ray diffractometry (XRD) was utilized to examine the crystalline properties of the membranes through D/Max-2500/PC. To gauge the hydrophobicity of the membranes, the water contact angle (WCA) – which was done at room temperature – was measured using a goniometer (SL200A by KINO Scientific Instrument Inc.,) while the moisture transmission rate (MTR) is determined as per the ASTM standard E96 [30]. The oxygen and nitrogen permeability and selectivity of all membranes have been studied to evaluate whether this membrane is suitable for LAB or not. The oxygen and nitrogen permeability and selectivity were measured with the help of a gas separation setup. The permeability was calculated from the volume flow rate and pressure difference.

$$P = \frac{Q \times l}{A \times PD}, \tag{3}$$

where P is the permeability of the membrane for a particular gas, Q is the flow rate of the gas, l is the thickness of the membrane, A is the cross sectional area of the membrane and PD is the pressure difference across the membrane.

The selectivity of the membrane was characterized as

$$\alpha = \frac{P_{O_2}}{P_{N_2}}, \tag{4}$$

where α is the selectivity of the gas.

For the electrochemical characterization various tests were conducted. Cyclic voltammetry (CV) and electrochemical impedance spectroscopy (EIS) were used on the cathode. Discharge/charge test of the battery was carried out using the CorrTest Electrochemical workstation.

3 Results and discussion

To analyze the functional groups in the prepared membranes, FTIR analysis was conducted of both pristine and graphite filled membranes (see Fig. 5). The peaks observed

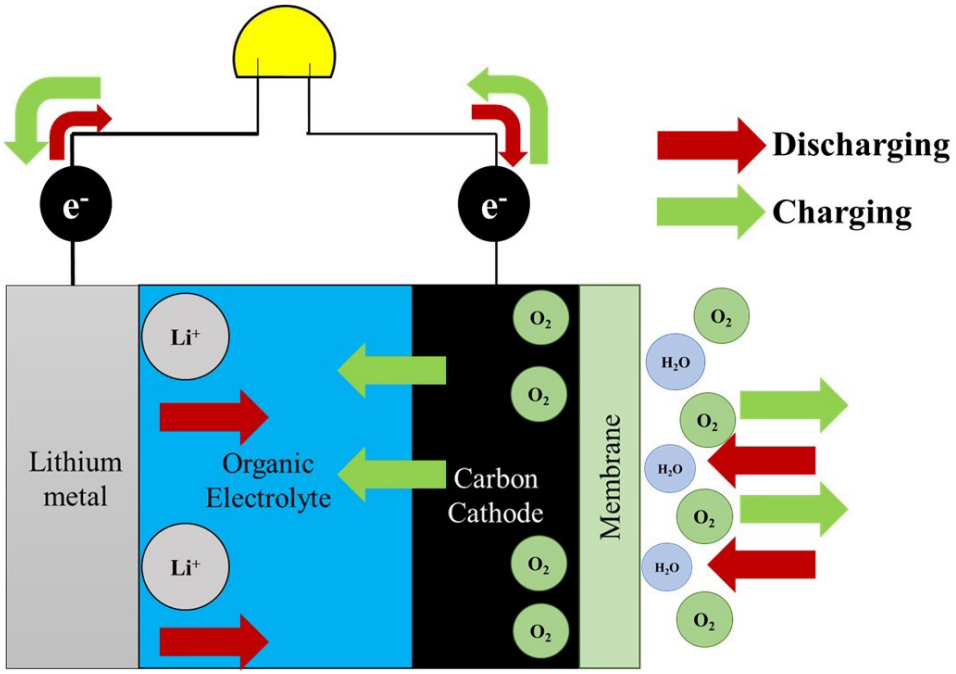

Fig. 4 Scheme of battery with a hydrophobic

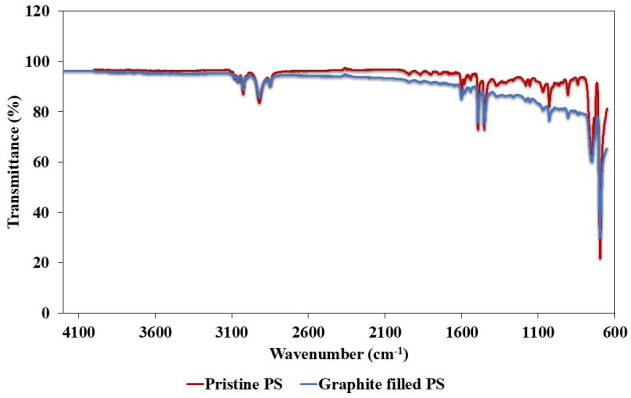

Fig 5 FTIR spectra of the prepared membranes

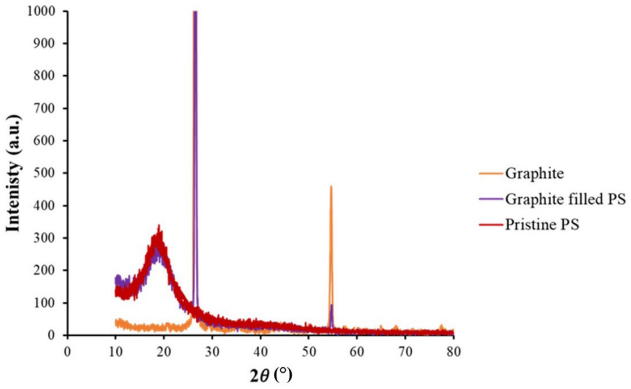

Fig 6 XRD of prepared membranes

in the range of 3100-2800 cm^{-1} show the symmetric and asymmetric vibrations of the C–H bond [31]. The aromatic C=C stretching vibration is evident from the peaks observed in 1600-1400 cm^{-1}, indicating the presence of a benzene ring. The peaks observed at wave numbers 747 and 695 cm^{-1} confirm the existence of out-of-plane C–H bonding and signal a substitution on the benzene ring. These findings align well with the research published in reference [31]. Both pristine and graphite filled membranes exhibit these peaks, but the graphite filled membrane displays a downward trend, reflecting the inert nature of graphite that does not produce any peaks in FTIR but instead results in a declining line, as noted in reference [32].

The analysis of the prepared membranes crystalline structure was conducted using XRD, and the findings are presented in Fig. 6. The presence of a broad peak at 2θ = 20.40° indicates the successful synthesis of the PS membrane, as reported in reference [31]. This broad peak is related to the amorphous nature of PS. Additionally, another distinct peak observed at approximately 26.4° confirms the presence of graphite within the PS matrix.

The morphology of the pristine PS membrane and 0.7 wt.% graphite filled PS membrane were analyzed using SEM by passing the electron beam at 20 kV and the results are presented in Fig. 7. The top view of the pristine membrane studied at a magnification of 2000X is shown in Fig. 7(a). Fig. 7(a) illustrates that the pristine membrane possessed a flat and smooth matrix. Fig. 7(b) reveals a uniform distribution of graphite within the PS matrix, signifying the successful creation of a composite membrane. When the quantity of graphite flakes was increased to 1 wt.% of PS, it is observed that graphite flakes are not able

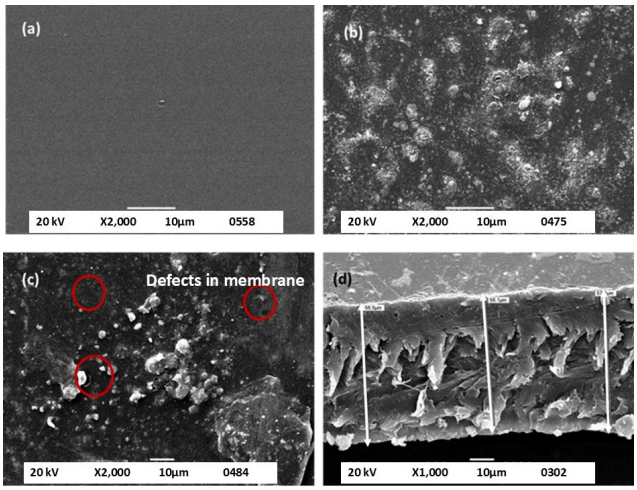

Fig. 7 (a) Top view of pristine PS membrane; (b) Top view of 0.7 wt% graphite filled PS membrane; (c) Top view of 1 wt% graphite filled PS membrane, where red circles indicate defects in membrane; (d) Cross-section of 0.7 wt% graphite filled PS membrane

to distribute uniformly within the matrix causing agglomeration and defects within the membrane as shown in Fig. 7(c). So, 1 wt.% of PS, graphite flakes are not suitable for membrane preparation. The 0.7 wt.% graphite filled PS membrane is also free from defects. Graphite turns the membrane surface to be rough, while it is smooth in the pristine one. The cross-section of the prepared membrane was studied at a magnification of 1000X and the result is presented in Fig. 7(d). From a cross-sectional view, it is evident that the prepared membrane has a uniform thickness of around 56.8 µm. The orientation of graphite flakes within the membrane is inclined. Due to the inclined orientation of graphite flakes within the matrix, it is effective in moisture blocking [33], because it takes a longer path for the moisture to diffuse through the composite membrane as compared to the pristine one.

The hydrophobicity of the prepared membranes was analyzed by determining the WCA of all the prepared membranes. The images are presented in Fig. 8. It is clear from the images that the contact angle of the pristine PS membrane was 88° which was further increased to 93° when the 0.3 wt.% graphite was added to the matrix. It means that the addition of graphite is favorable in increasing the WCA. After further increasing the quantity of graphite to 0.5 wt.%, WCA was further increased to 99°. When the graphite was further increased to 0.7 wt.% WCA angle is further increased to 109° which is observed to be the best WCA among all the prepared membranes: when the graphite was further increased to 1 wt.% of PS, the WCA declined to 103.2°. It means that by increasing the quantity of graphite within the PS matrix, the hydrophobicity first increased up to a maximum value and then

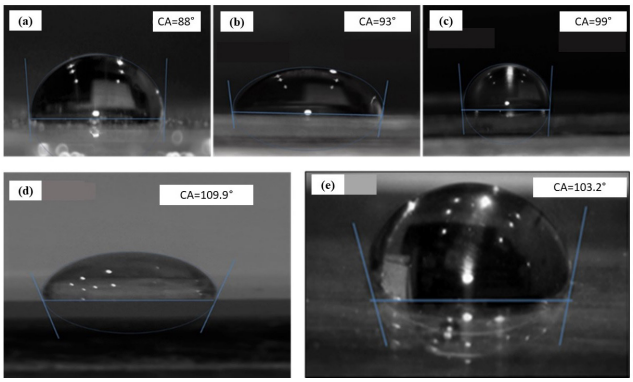

Fig. 8 Water contact angle (a) pristine PS, (b) 0.3 wt% graphite filled PS membrane, (c) 0.5 wt% graphite filled PS membrane, (d) 0.7 wt% graphite filled PS membrane, (e) 1 wt% graphite filled PS membrane

declined. Among all the prepared membranes, 0.7 wt.% of PS filled with graphite showed the highest hydrophobicity. The hydrophobicity was increasing by increasing the quantity of graphite because the composite membranes seem to be rough as compared to the pristine one, which in turn increased the WCA, which means that the hydrophobicity increased.

The prepared membranes were tested to evaluate their ability to block moisture permeation. Fig. 9(a) provides a visual representation of the experimental setup for MTR determination according to ASTM standard E96. In this setup, the membrane is positioned over a beaker filled with distilled water. Initially, the combined mass of the water filled cup and the membrane was measured, and then they were left undisturbed for seven days at room temperature. Each day, the mass of the cup was recorded, and subsequently, the MTR was calculated using Eq. (5).

$$MTR = \frac{W_1 - W_2}{A \times t} \tag{5}$$

Here, W_1 is the initial mass of the container, W_2 is the final mass of the container and t is the time. The results of MTR are presented in Fig. 9(b). It is clear that the pristine PS membrane has an MTR of 0.51 g/(m^2 × day). When the graphite was added to the PS matrix, MTR decreased. The 0.3 wt.% graphite filled PS membrane showed an MTR of 0.32 g/(m^2 × day), which means that the addition of graphite is favorable in moisture blocking. When the graphite was further increased to 0.5 wt.%, MTR further decreased to 0.2 g/(m^2 × day). After further increasing the quantity of graphite to 0.7 wt.% of PS, the same trend is observed and MTR decreased to 0.12 g/(m^2 × day). When the quantity of graphite was further increased to 1 wt.% of PS, further decrement of MTR was not observed and MTR jumped to around 0.22 g/(m^2 × day).

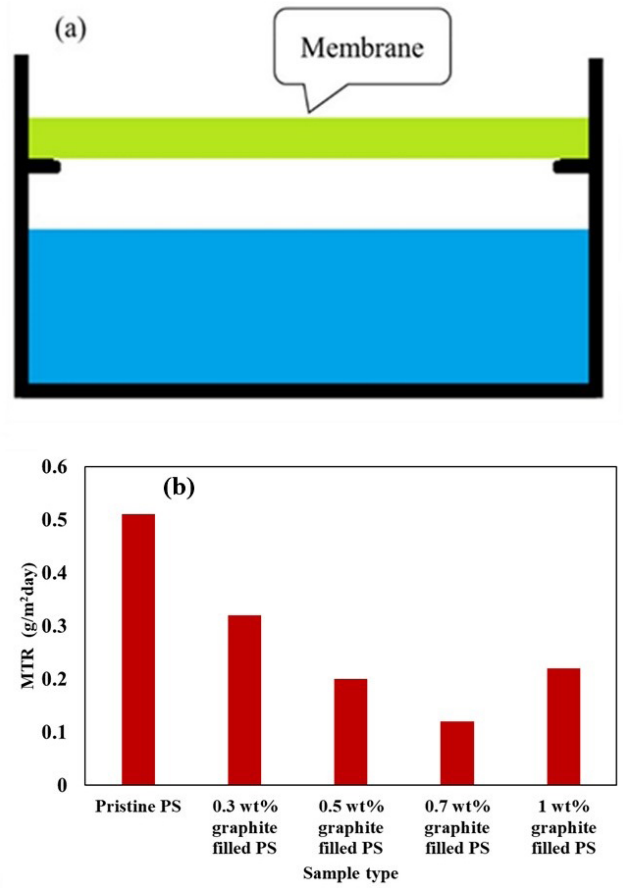

Fig. 9 (a) Scheme of the MTR setup, (b) MTR values of all the prepared membranes

It means that the addition of graphite to PS is effective in increasing MTR but after giving the optimum results, the MTR is starting to decline. This occurs because defects were formed in the membrane when the quantity of graphite flakes was increased as evident from the SEM image in Fig. 7 (red circles).

The results of oxygen and nitrogen permeability and selectivity are presented in Fig. 10. Four membranes including pristine, 0.3 wt%, 0.5 wt% and 0.7 wt% graphite in PS were selected to study the gas separation ability. 1 wt% was not considered because of its lower resistance in moisture transmission. According to the results, by the introduction of graphite flakes in the PS membrane, the selectivity of the oxygen is increasing while the permeability is decreasing due to the Robenson limit [34]. From Fig. 10(a), the permeability of oxygen gas is 183, 142, 67, and 35 barrers for pristine, 0.3 wt%, 0.5 wt%, and 0.7 wt% of PS graphite filled membranes, while the nitrogen permeability were found to be 153, 77, 23 and 8.5 barrers respectively. From Fig. 10(b), the O_2/N_2 selectivity for the pristine membrane was reported to be 1.2, while for the membrane containing 0.3 wt% graphite in PS the O_2/N_2 selectivity improved to 1.87. Upon further increasing the amount of graphite flakes up to 0.5 wt% of PS, the O_2/N_2 selectivity increased to 3.02 which was further improved to 4.05 when the quantity of graphite flakes was increased to 0.7 wt%. From these results, it can be concluded that graphite flakes present in the matrix of PS support the diffusion of oxygen molecules more as compared to nitrogen molecules, therefore the O_2/N_2 selectivity is increasing. The increase in O_2/N_2 selectivity occurs because graphite shows affinity towards oxygen due to which oxygen diffuses faster than that of nitrogen. The mechanism of the graphite-oxygen interaction is quite complex. A fundamental knowledge about the crystal structure of graphite along with the anisotropy is required to completely comprehend the difficulty. The carbon basal planes in graphite have strong directed covalent sp^2 hybridized bonding (002) which are linked together by weak van der Waals forces among the planes. It results in very weak

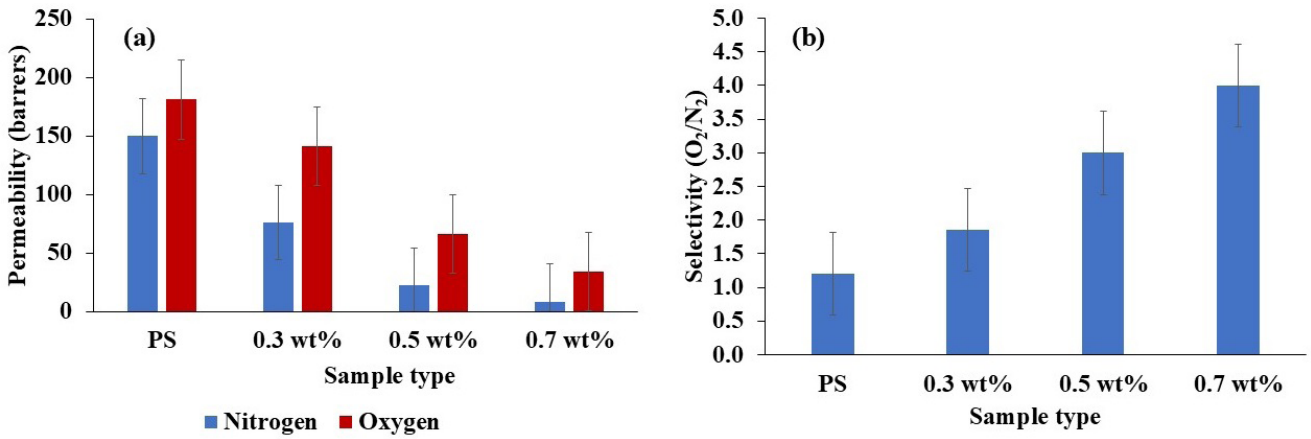

Fig. 10 (a) Oxygen and nitrogen permeability (1 barrer = 3.35×10^{-16} mol × m/(m² × s × Pa)); (b) Selectivity of oxygen over nitrogen (for detailed description of sample type see the horizontal axis in Fig. 9(b))

chemical interactions between planes [35]. This resulted in the piling of oxygen in the membrane and, eventually, due to the upstream of the oxygen, they were forced to cross the membrane faster as compared to nitrogen. This result can enable the 0.7 wt% graphite-filled membrane to be used in LABs.

The CV of the prepared cathodes was used to study the oxygen reduction reaction (ORR) and oxygen evolution reaction (OER). The results are presented in Fig. 11. The CV was conducted in 0.1 M aqueous solution of KOH saturated with oxygen at a scanning rate of 10 mV/s. Graphite was used as the counter electrode, while Ag/AgCl was used as reference electrode.

From Fig. 11, it is evident that for the cathode without MnO_2 the cathodic peak was observed at 0.38 V and 0.06 A, while no anodic peak was observed for the cathode with MnO_2. This indicates that without MnO_2 the battery can be recharged to a small extent as no electrochemical reaction is observed. Without any electrochemical reaction, the battery can not reach its initial state. When MnO_2 was added to the cathode, the cathodic peak was observed at 0.29 V and 0.014 A. Very little bump as an anodic peak (blue line) at around 0.65 V and 0.01 A was observed for the cathode with MnO_2. This peak is observed because of the insertion of proton into MnO_2 according to Eq. (6) [36]. This little bump is an indication that some electrochemical reaction occurred, however, the relatively low intensity of the anodic peak suggests limited reversibility and, consequently, poor cyclability of the cell. This limitation, however, does not affect the primary objective of the present study, which is to investigate the influence of membrane incorporation on the performance of the lithium-air battery (LAB) under moist-air operating conditions.

$$MnO_2 + H_2O + e^- \rightarrow MnOOH + OH^- \quad (6)$$

The charge transfer resistance of the cathode was investigated using electrochemical impedance spectroscopy (EIS), employing Graphite as the counter electrode and Ag/AgCl as the reference electrode in an oxygen-saturated 0.1 M KOH solution. This test covered a frequency range from 0.01 Hz to 1 MHz (see Fig. 12). In the absence of a catalyst, the charge transfer resistance was measured at 2.3 W, while the overall cell resistance is 5.2 W. When MnO_2 is introduced as catalyst, the charge transfer resistance decreased to 1.2 W, and the cell resistance decreased to 4.9 W. The notable reduction in both parameters highlights the catalytic activity of MnO_2, which accelerates the electrochemical reactions by facilitating faster electron transfer and enhancing ion diffusion at the cathode surface. This improvement reflects an overall enhancement in the electrochemical performance of the cell, demonstrating that MnO_2 effectively promotes the oxygen reduction process and reduces the interfacial resistance, ultimately contributing to better cathode efficiency and stability. Furthermore, MnO_2 introduces oxygen vacancies, further reducing the overall resistance of the cathode and enhancing its performance [37]. This means that ORR will be faster because the charge transfer process is faster. The nanorod structure of MnO_2 plays a significant role in supporting the electrode-electrolyte interface of the cathode and enhancing electron conductivity [38]. The addition of MnO_2 as a catalyst within the cathode material proved to be beneficial in lowering the overall resistance of the battery and enhancing its performance.

To assess the impact of the membranes on LAB performance, tests were conducted both with and without the membrane. The LAB lacking a membrane was assembled within an argon filled glove box, resulting in an open circuit voltage of approximately 1.9 V, as depicted in Fig. 13. To determine the total capacity of the battery, it was

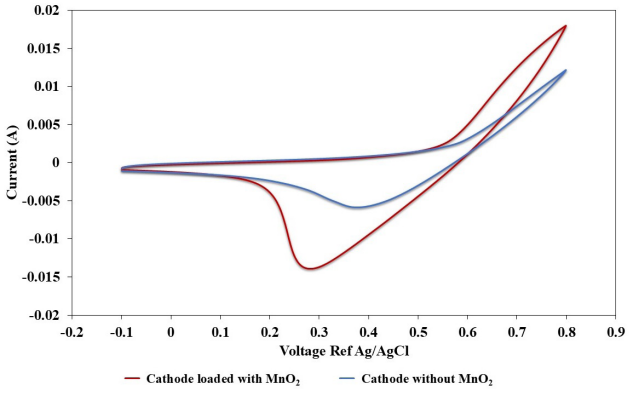

Fig. 11 Cyclic voltammetry (CV) of the prepared cathodes

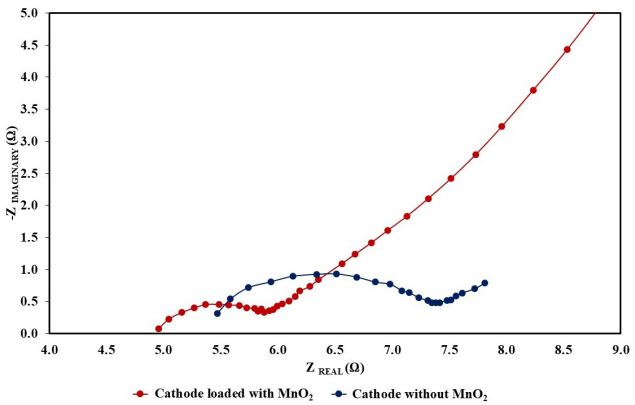

Fig. 12 EIS of the prepared cathode

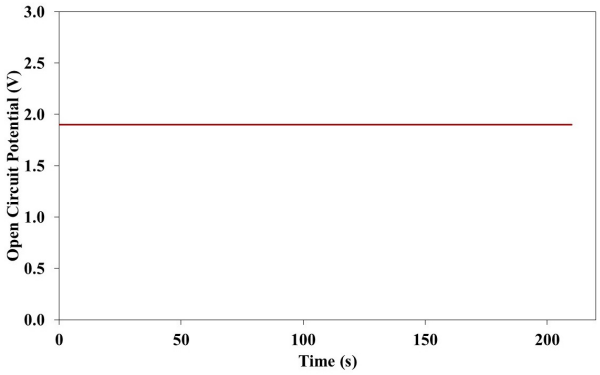

Fig. 13 Open circuit potential of battery with PC as electrolyte

discharged entirely within oxygen environment at a discharge rate of 1.5 mA/g. The results indicated that the battery achieved a discharge capacity of roughly 1058 mAh/g in a pure oxygen environment, delivering a voltage of 1.8 V, as illustrated by the red curve in Fig. 14. The discharge voltage of the battery is different from the open circuit voltage because when the battery is connected to the battery tester, there may be losses due to ohmic losses or internal resistance of the battery, which can be studied separately.

The low voltage of the cell can be attributed to inadequate contact between the electrode and the test cell. However, in the context of this study, this issue is not deemed critical since the primary objective is to assess the influence of the membrane on the battery performance. To investigate the impact of the membrane on the LAB discharge capacity, a battery containing a 0.7 wt.% graphite filled membrane is assembled within an argon filled glove box. Subsequently, the battery underwent discharge at the same rate of 1.5 mA/g, first in pure oxygen environment and then using a stream of moist gas. Based on the findings from WCA and MTR measurements, the 0.7 wt.% graphite filled PS membrane

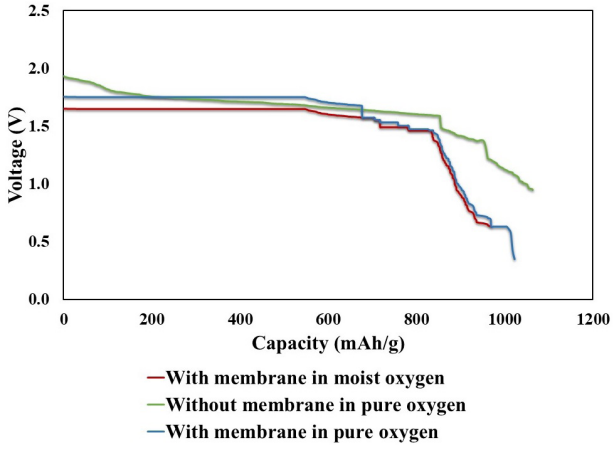

Fig. 14 Discharge capacity of the battery without and with membrane

demonstrated the most promising performance as a moisture barrier. Consequently, it was selected for incorporation into the membrane for moisture prevention.

At first, when the battery with the membrane was discharged in pure oxygen, it provided the maximum capacity of 1022 mAh/g at the same rate as evidenced by the green curve in Fig. 14. The low capacity was observed because the membrane caused resistance in the oxygen flow and the performance of the battery was strongly dependent on the oxygen partial pressure [39]. After studying the battery performance with the membrane in pure oxygen another battery with 0.7 wt.% graphite filled membrane was assembled and then discharged by using a stream of moist gas to study the effectiveness of the membrane in moisture blocking. The moist gas was used to simulate the ambient conditions as ambient conditions also include moisture. The stream of gas used consisted of around 14% moisture and 86% oxygen. When a battery equipped with the membrane was discharged in moist gas, it behaved in the same way as the battery performed in pure oxygen environment. The discharge capacity of the battery equipped with membrane when discharge in the moist gas was found to be around 981 mA/g as evidenced by the purple curve of Fig. 14. The battery provided the above-mentioned capacity because it is supposed for all the studied batteries that during the discharge operation first an electrochemical reaction between oxygen and lithium occurs and Li_2O_2 is formed as a discharged product. However, due to the presence of the carbonate based electrolyte, this discharged product can be transformed into Li_2CO_3 according to Eq. (7). The carbonate based discharge product is assumed to get stuck on the surface of the cathode and ultimately resulted in clogging of the cathode, due to which there are no active sites available for further electrochemical reaction. The discharge capacity can be enhanced by using a cathode with a high surface area and more active sites, because high surface area means more active sites for electrochemical reactions.

$$Li_2O_2 + CO_3^{-2} \rightarrow Li_2CO_3 + 2O^{-2} \quad (7)$$

From the discharge operation, it is also found that there is no safety issue during the operation of the battery with moist gas. When the membrane is used for moisture blocking, as shown in Fig. 15, the lithium coin is found to be in a better state as compared to the other. The discharge capacity of a battery with a membrane was found to be lower than that of a battery without a membrane, because

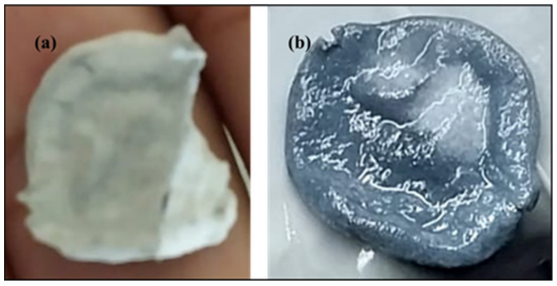

Fig. 15 (a) Lithium coin after exposure to moist gas, (b) Lithium coin from a battery with membrane after discharging in moist gas

the membrane creates a hindrance in the flow of oxygen and thus reduces the pressure of oxygen in the battery. The capacity of the battery performance is highly dependent on the oxygen pressure [39].

Fig. 16 shows the cyclic discharge and charge performance of LAB in pure oxygen without a membrane and in an oxygen environment and moist gas with a membrane. The moist gas is composed of around 14% moisture and 86% oxygen. The battery was discharged by setting the capacity to 500 mAh/g. The battery was discharged and charged at a rate of around 1.5 mA/g. During the first cycle, the battery with and without membrane provided the same capacity which is fixed initially. However, after the first cycle, the battery capacity decreased continuously. It is evident from Fig. 16 that in every following cycle, the battery provided a lesser capacity than the previous one and gradually the overpotential continuously increased. In all three scenarios, LAB just lasted for 7 cycles. The lower capacity may be caused by the polycarbonate electrolyte. Carbonate electrolytes, in general, react with the discharge product Li_2O_2 and form Li_2CO_3. It is difficult to decompose and deposits on the cathode, thus decreasing the performance of the battery [40]. The battery capacity may be enhanced by replacing the carbonate based electrolyte with tetraethylene glycol dimethyl ether (TEGDME). A sudden overshoot was observed in the last cycle of the battery without membrane because, during the battery operation, the temperature of the battery increased and the electrolyte evaporated. It can also be concluded that at the end of the 7th cycle, the battery ended not only because of carbonate formation but also due to the evaporation of the electrolyte.

However, in the battery with a membrane, the electrolyte evaporation was restricted by the membrane due to which a gradual decrement was observed. It can also be said that the battery with a membrane performed better because in the battery with a membrane the shortening of battery life is mainly due to the carbonate formation and the electrolyte evaporation is negligible.

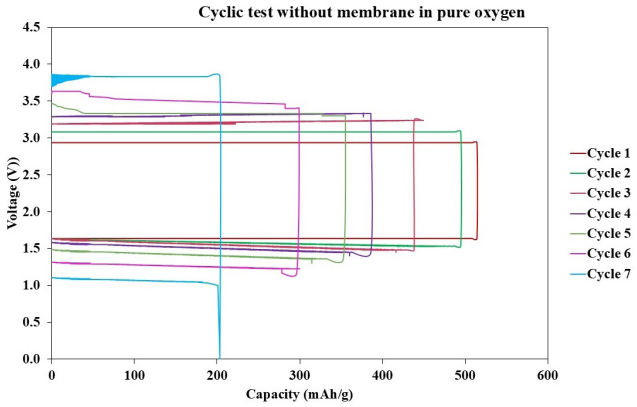

(a)

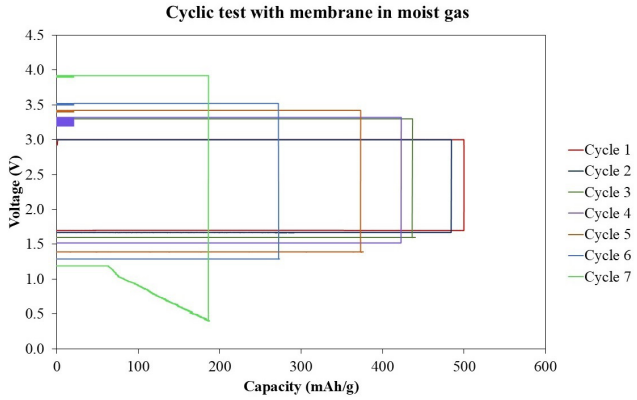

(b)

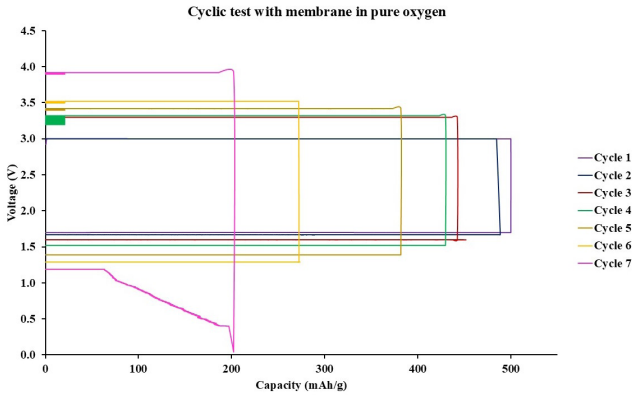

(c)

Fig. 16 Cyclic Performance of battery (a) without membrane in pure oxygen, (b) with the membrane in moist gas, (c) with the membrane in pure oxygen

4 Conclusion

To ensure the safe and reliable operation of LABs in ambient conditions, it has been determined that hydrophobic membranes represent the optimal choice. These membranes effectively prevent moisture ingress while permitting the passage of oxygen into the battery. In this context, a polystyrene based membrane was successfully

synthesized and comprehensively characterized using techniques such as FTIR, XRD, SEM, WCA and MTR. The most effective PS-based membrane, identified through these analyses, was subsequently employed in the battery to serve as a moisture barrier. The following research findings are drawn from this investigation:

- The optimum quantity of graphite within in PS matrix is 0.7 wt.% of PS. Among all the prepared membranes, 0.7 wt.% graphite filled PS membrane has performed the best in restricting moisture and also has the highest WCA, which means high hydrophobicity.
- Incorporating MnO_2 as a catalyst in the cathode material yielded positive outcomes, reducing the overall resistance and allowing multiple cycle cathode use.
- The utilization of a 0.7 wt.% graphite filled PS membrane proved to be effective for operating the battery under ambient conditions. While this research employed moist gas, it effectively simulated real-world ambient conditions. The 0.7 wt.% graphite filled PS membrane enabled the battery to deliver capacity on par with the original battery while safeguarding the lithium anode during operation.

Although the battery underwent only seven cycles, our research primarily aimed to investigate the performance of a battery equipped with a PS-based membrane in ambient conditions. It is observed that the battery with the membrane, tested in moist gas, performed comparably to a battery without a membrane tested in a pure oxygen environment. Enhancing the cyclic performance of the battery can be achieved by substituting the carbonate based electrolyte with TEGDME.

References

[1] Sun, Q., Dai, L., Luo, T., Wang. L., Liang, F., Liu, S. "Recent advances in solid-state metal–air batteries", Carbon Energy, 5(2), e276, 2023. https://doi.org/10.1002/cey2.276

[2] Girishkumar, G., McCloskey, B., Luntz, A. C., Swanson, S., Wilcke, W. "Lithium-air battery: Promise and challenges", The Journal of Physical Chemistry Letters, 1(14), pp. 2193–2203, 2010. https://doi.org/10.1021/jz1005384

[3] Abraham, K. M., Jiang, Z. "A Polymer Electrolyte-Based Rechargeable Lithium / Oxygen Battery", Journal of The Electrochemical Society, 143(1), pp. 1–5, 1996. https://doi.org/10.1149/1.1836378

[4] Bi, X., Jiang, Y., Chen, R., Du, Y., Zheng, Y., Yang, R., Wang, R., Wang, J., Wang, X., Chen, Z. "Rechargeable Zinc–Air versus Lithium–Air Battery: from Fundamental Promises Toward Technological Potentials", Advanced Energy Materials, 14(6), 2302388, 2024. https://doi.org/10.1002/aenm.202302388

[5] Zhang, Z., Xiao, X., Zhu, X., Tan, P. "Addressing Transport Issues in Non-Aqueous Li–air Batteries to Achieving High Electrochemical Performance", Electrochemical Energy Reviews, 6(1), 18, 2023. https://doi.org/10.1007/s41918-022-00157-3

[6] Freunberger, S. A., Chen, Y., Drewett, N. E., Hardwick, L. J., Bardé, F., Bruce, P. G. "The lithium-oxygen battery with ether-based electrolytes", Angewandte Chemie - International Edition, 50(37), pp. 8609–8613, 2011. https://doi.org/10.1002/anie.201102357

[7] Mirzaeian, M., Hall, P. J. "Characterizing capacity loss of lithium oxygen batteries by impedance spectroscopy", Journal of Power Sources, 195(19), pp. 6817–6824, 2010. https://doi.org/10.1016/j.jpowsour.2010.04.064

[8] Zahoor, A., Jang, H. S., Jeong, J. S., Christy, M., Hwang, Y. J., Nahm, K. S. "A comparative study of nanostructured α and δ MnO_2 for lithium oxygen battery application", RSC Advances, 4(18), pp. 8973–8977, 2014. https://doi.org/10.1039/c3ra47659f

[9] Asad, S., Zahoor, A., Butt, F. A., Hashmi, S., Raza, F., …, Christy, M. "Recent Advances in Titanium Carbide MXene ($Ti_3C_2T_x$) Cathode Material for Lithium-Air Battery", ACS Applied Energy Materials, 5(10), pp. 11933–11946, 2022. https://doi.org/10.1021/acsaem.2c01845

[10] Ogasawara, T., Débart, A., Holzapfel, M., Novák, P., Bruce, P. G. "Rechargeable Li_2O_2 electrode for lithium batteries", Journal of the American Chemical Society, 128(4), pp. 1390–1393, 2006. https://doi.org/10.1021/ja056811q

[11] He, P., Zhang, T., Jiang, J., Zhou, H. "Lithium-Air Batteries with Hybrid Electrolytes", The Journal of Physical Chemistry Letters, 7(7), pp. 1267–1280, 2016. https://doi.org/10.1021/acs.jpclett.6b00080

[12] Lu, J., Lee, Y. J., Luo, X., Lau, K. C., Asadi, M., …, Amine, K. "A lithium-oxygen battery based on lithium superoxide", Nature, 529(7586), pp. 377–382, 2016. https://doi.org/10.1038/nature16484

[13] Wang, Z., Chen, X., Shen, F., Hang, X., Niu, C. "TiC MXene High Energy Density Cathode for Lithium–Air Battery", Advanced Theory and Simulations, 1(9), 1800059, 2018. https://doi.org/10.1002/adts.201800059

[14] Kang, J. "An ultrahigh power Li–O_2 battery", Materials Today: Communication, 27, 102412, 2021. https://doi.org/10.1016/j.mtcomm.2021.102412

[15] Ottakam Thotiyl, M. M., Freunberger, S. A., Peng, Z., Chen, Y., Liu, Z., Bruce, P. G. "A stable cathode for the aprotic Li-O_2 battery", Nature Materials, 12(11), pp. 1050–1056, 2013. https://doi.org/10.1038/nmat3737

[16] Naqvi, A. A., Zahoor, A., Shaikh, A. A., Butt, F. A., Raza, F., Ahad, I. U. "Aprotic lithium air batteries with oxygen-selective membranes", Materials for Renewable and Sustainable Energy, 11(1), pp. 33–46, 2022. https://doi.org/10.1007/s40243-021-00205-w

[17] Masters, G. M. "Renewable and Efficient Electric Power Systems", John Wiley & Sons, 2004. ISBN 9780471668824 https://doi.org/10.1002/0471668826

[18] Zou, X., Lu, Q., Liao, K., Shao, Z. "Towards practically accessible aprotic Li-air batteries: Progress and challenges related to oxygen-permeable membranes and cathodes", Energy Storage Materials, 45, pp. 869–902, 2022. https://doi.org/10.1016/j.ensm.2021.12.031

[19] Huang, S., Cui, Z., Zhao, N., Sun, J., Guo, X. "Influence of Ambient Air on Cell Reactions of Li-air Batteries", Electrochimica Acta, 191, pp. 473–478, 2016. https://doi.org/10.1016/j.electacta.2016.01.102

[20] Crowther, O., Salomon, M. "Oxygen selective membranes for Li-air (O_2) batteries", Membranes, 2(2), pp. 216–227, 2012. https://doi.org/10.3390/membranes2020216

[21] Muthiah, P., Hsu, S.-H., Sigmund, W. "Coaxially electrospun PVDF-teflon AF and teflon AF-PVDF core-sheath nanofiber mats with superhydrophobic properties", Langmuir, 26, (15), pp. 12483–12487, 2010. https://doi.org/10.1021/la100748g

[22] Crowther, O., Keeny, D., Moureau, D. M., Meyer, B., Salomona, M., Hendrickson, M. "Electrolyte optimization for the primary lithium metal air battery using anoxygen selective membranes", Journal of Power Sources, 202, pp. 347–351, 2012. https://doi.org/10.1016/j.jpowsour.2011.11.024

[23] Zhang, J. G., Wang, D., Xu, W., Xiao, J., Williford, R. E. "Ambient operation of Li/Air batteries", Journal of Power Sources, 195(13), pp. 4332–4337, 2010. https://doi.org/10.1016/j.jpowsour.2010.01.022

[24] Zou, X., Liao, K., Wang, D., Lu, Q., Zhou, C., He, P., Ran, R., Zhou, W., Jin, W., Shao, Z. "Water-proof, electrolyte-nonvolatile, and flexible Li-Air batteries via O_2-Permeable silica-aerogel-reinforced polydimethylsiloxane external membranes", Energy Storage Materials, 27, pp. 297–306, 2020. https://doi.org/10.1016/j.ensm.2020.02.014

[25] Xie, M., Huang, Z., Lin, X., Li, Y., Huang, Z., Yuan, L., Shen, Y., Huang, Y. "Oxygen selective membrane based on perfluoropolyether for Li-Air battery with long cycle life", Energy Storage Materials, 20, pp. 307–314, 2019. https://doi.org/10.1016/j.ensm.2018.11.023

[26] Zhang, J., Xu, W., Li, X., Liu, W. "Air Dehydration Membranes for Nonaqueous Lithium–Air Batteries", Journal of The Electrochemical Society, 157(8), A940, 2010. https://doi.org/10.1149/1.3430093

[27] Fu, Z., Wei, Z., Lin, X., Huang, T., Yu, A. "Polyaniline membranes as waterproof barriers for lithium air batteries", Electrochimica Acta, 78, pp. 195–199, 2012. https://doi.org/10.1016/j.electacta.2012.05.153

[28] Wen, X., Zhu, X., Wu, Y., Wang, Y., Man, Z., Lv, Z., Wang, X. "A hydrophobic membrane to enable lithium-air batteries to operate in ambient air with a long cycle life", Electrochimica Acta, 421, 140517, 2022. https://doi.org/10.1016/j.electacta.2022.140517

[29] Wang, J., Ke, Y., Chen, X., Jia, Z. "Preparation of Waterproof and Air-Permeable Membrane by Water Surface Spreading Method for Metal-Air Battery", ACS Sustainable Chemistry & Engineering, 10(9), pp. 2903–2913, 2022. https://doi.org/10.1021/acssuschemeng.1c07526

[30] ASTM "ASTM E96/E96M–05 Standard Test Methods for Water Vapor Transmission of Materials", ASTM International, West Conshohocken, PA, USA, 1995.

[31] Fang, J., Xuan, Y., Li, Q. "Preparation of polystyrene spheres in different particle sizes and assembly of the PS colloidal crystals", Science China Technological Sciences, 53(11), pp. 3088–3093, 2010. https://doi.org/10.1007/s11431-010-4110-5

[32] Verma, P., Chowdhury, R., Chakrabarti, A. "Role of graphene-based materials (GO) in improving physicochemical properties of cementitious nano-composites: a review", Journal of Materials Science, 56(35), pp. 19329–19358, 2021. https://doi.org/10.1007/s10853-021-06526-5

[33] Bharadwaj, R. K. "Modeling the barrier properties of polymer-layered silicate nanocomposites", Macromolecules, 34(26), pp. 9189–9192, 2001. https://doi.org/10.1021/ma010780b

[34] Robeson, L. M. "Correlation of separation factor versus permeability for polymeric membranes", Journal of Membrane Science, 62(2), pp. 165–185, 1991. https://doi.org/10.1016/0376-7388(91)80060-J

[35] Kane, J. J., Contescu, C. I., Smith, R. E., Strydom, G., Windes, W. E. "Understanding the reaction of nuclear graphite with molecular oxygen: Kinetics, transport, and structural evolution", Journal of Nuclear Materials, 493, pp. 343–367, 2017. https://doi.org/10.1016/j.jnucmat.2017.06.001

[36] Khilari, S., Pandit, S., Ghangrekar, M. M., Das, D., Pradhan, D. "Graphene supported α-MnO_2 nanotubes as a cathode catalyst for improved power generation and wastewater treatment in single-chambered microbial fuel cells", RSC Advances, 3(21), pp. 7902–7911, 2013. https://doi.org/10.1039/c3ra22569k

[37] Zhang, Y., Liu, Y., Liu, Z., Wu, X., Wen, Y., Chen, H., Ni, X., Liu, G., Huang, J., Peng, S. "MnO_2 cathode materials with the improved stability via nitrogen doping for aqueous zinc-ion batteries", Journal of Energy Chemistry, 64, pp. 23–32, 2022. https://doi.org/10.1016/j.jechem.2021.04.046

[38] Pandit, B. Rondiya, S. R., Shaikh, S. F., Ubaidullah, R. A., Dzade, N. Y., Goda, E. S., ul Hassan Sarwar Rana, A., Singh Gill, H., Ahmad, T. "Regulated electrochemical performance of manganese oxide cathode for potassium-ion batteries: A combined experimental and first-principles density functional theory (DFT) investigation", Journal of Colloid and Interface Science, 633, pp. 886–896, 2023. https://doi.org/10.1016/j.jcis.2022.11.070

[39] Kwon, H. J., Lee, H. C., Ko, J., Jung, I. S., Lee, H. C., …, Im, D. "Effects of oxygen partial pressure on Li-air battery performance", Journal of Power Sources, 364, pp. 280–287, 2017. https://doi.org/10.1016/j.jpowsour.2017.08.052

[40] Zhao, Z., Huang, J., Peng, Z. "Achilles' Heel of Lithium–Air Batteries: Lithium Carbonate", Angewandte Chemie - International Edition, 57(15), pp. 3874–3886, 2018. https://doi.org/10.1002/anie.201710156